



OPEN

Hypersensitivity of myelinated A-fibers via toll-like receptor 5 promotes mechanical allodynia in tenascin-X-deficient mice associated with Ehlers–Danlos syndrome

Hiroki Kamada¹, Kousuke Emura¹, Rikuto Yamamoto¹, Koichi Kawahara¹, Sadahito Uto¹, Toshiaki Minami², Seiji Ito², Ken-ichi Matsumoto³ & Emiko Okuda-Ashitaka¹✉

Deficiency of an extracellular matrix glycoprotein tenascin-X (TNX) leads to a human heritable disorder Ehlers–Danlos syndrome, and TNX-deficient patients complain of chronic joint pain, myalgia, paresthesia, and axonal polyneuropathy. We previously reported that TNX-deficient (*Tnxb*^{-/-}) mice exhibit mechanical allodynia and hypersensitivity to myelinated A-fibers. Here, we investigated the pain response of *Tnxb*^{-/-} mice using pharmacological silencing of A-fibers with co-injection of *N*-(2,6-Dimethylphenylcarbonylmethyl) triethylammonium bromide (QX-314), a membrane-impermeable lidocaine analog, plus flagellin, a toll-like receptor 5 (TLR5) ligand. Intraplantar co-injection of QX-314 and flagellin significantly increased the paw withdrawal threshold to transcutaneous sine wave stimuli at frequencies of 250 Hz (A δ fiber responses) and 2000 Hz (A β fiber responses), but not 5 Hz (C fiber responses) in wild-type mice. The QX-314 plus flagellin-induced silencing of A δ - and A β -fibers was also observed in *Tnxb*^{-/-} mice. Co-injection of QX-314 and flagellin significantly inhibited the mechanical allodynia and neuronal activation of the spinal dorsal horn in *Tnxb*^{-/-} mice. Interestingly, QX-314 alone inhibited the mechanical allodynia in *Tnxb*^{-/-} mice, and it increased the paw withdrawal threshold to stimuli at frequencies of 250 Hz and 2000 Hz in *Tnxb*^{-/-} mice, but not in wild-type mice. The inhibition of mechanical allodynia induced by QX-314 alone was blocked by intraplantar injection of a TLR5 antagonist TH1020 in *Tnxb*^{-/-} mice. These results suggest that mechanical allodynia due to TNX deficiency is caused by the hypersensitivity of A δ - and A β -fibers, and it is induced by constitutive activation of TLR5.

Tenascin-X (TNX) is an extracellular matrix glycoprotein, and TNX deficiency caused by compound heterozygous and homozygous mutations of the gene leads to a heritable connective tissues disorder Ehlers–Danlos syndrome (EDS)^{1–5}. EDS is characterized by hyperextensibility of skin, hypermobility of joints, and fragility of various connective tissues. In addition, pain is a severe clinical manifestation of EDS patients, and approximately 90% of EDS patients complain of chronic pain^{6–8}. EDS patients suffer from chronic neuropathic pain, generalized body pain, gastrointestinal pain, headache, dysmenorrhea, and fatigue, in addition to connective tissues-related pain such as joint pain, soft-tissue pain, and dislocations^{6,7}. TNX-deficient EDS patients complain of chronic pain such as chronic joint pain, myalgia, abdominal pain, fatigue, paresthesia, and axonal polyneuropathy^{3,5}. We have previously reported the pain behaviors of TNX-deficient (*Tnxb*^{-/-}) mice as a murine EDS model⁹. *Tnxb*^{-/-} mice exhibited increased sensitivity to innocuous mechanical stimuli, which is called mechanical allodynia, a major feature of neuropathic pain. *Tnxb*^{-/-} mice also showed significant hypersensitivity to transcutaneous sine wave

¹Department of Biomedical Engineering, Osaka Institute of Technology, Osaka 535-8585, Japan. ²Department of Anesthesiology, Osaka Medical and Pharmaceutical University, Takatsuki 569-8686, Japan. ³Department of Biosignaling and Radioisotope Experiment, Interdisciplinary Center for Science Research, Head Office for Research and Academic Information, Shimane University, Izumo 693-8501, Japan. ✉email: emiko.ashitaka@oit.ac.jp

stimuli at frequencies of 250 Hz (myelinated A δ fiber responses) and 2000 Hz (myelinated A β fiber responses) using analysis of sensory afferent fiber responses to a sine wave electric stimulator. However, the hypersensitivity of myelinated A δ - and A β -fibers by which TNX deficiency complicates the mechanical allodynia remains unknown.

It has been reported that blocking A-fibers can be specifically achieved by using the toll-like receptor 5 (TLR5) ligand flagellin and the membrane-impermeable sodium channel blocker *N*-(2,6-Dimethylphenyl)carbamoylmethyl triethylammonium bromide (QX-314)¹⁰. Activation of TLR5 induced by flagellin results in neuronal entry of QX-314, provoking TLR5-dependent blockade of sodium currents, primarily in A β fibers. Intraplantar co-administration of flagellin and QX-314 suppressed mechanical allodynia in neuropathic pain models induced by chemotherapy, nerve injury, and diabetic neuropathy. On the other hand, blocking C-fibers can be specifically achieved using the transient receptor potential vanilloid 1 (TRPV1) ligand capsaicin and QX-314¹¹. Co-administration of capsaicin and QX-314 resulted in the neuronal entry of QX-314 through the ion channel TRPV1, provoking a blockade of C-fibers.

In the present study, we used fiber-specific blockade using co-injection of QX-314 with flagellin or capsaicin to *Tnxb*^{-/-} mice, in order to elucidate the correlation between TNX deficiency-induced hypersensitivity of myelinated A-fibers and the mechanical allodynia. We examined the combination of sensory afferent fiber responses to a sine wave electric stimulator and behavioral pharmacology in *Tnxb*^{-/-} mice injected with QX-314, flagellin, or capsaicin. We demonstrated that TNX-deficiency-induced mechanical allodynia is mediated by A-fiber hypersensitivity, and that QX-314 alone-inhibited mechanical allodynia is mediated by constitutive activation of TLR5 in *Tnxb*^{-/-} mice.

Results

Sensory fiber-specific silencing in vivo in wild-type mice

We used pharmacological A-fiber silencing by intraplantar co-injection of the membrane-impermeable sodium channel blocker QX-314 and the TLR5 ligand flagellin, and C-fiber silencing by QX-314 and the TRPV1 ligand capsaicin. Intraplantar application of QX-314 (2%, approximately 60 mM, 20 μ L) with flagellin (0.3 μ g in 20 μ L) suppressed A-fiber conduction in naive and chemotherapy-treated mice, and application of QX-314 (0.2%, approximately 6 mM) with flagellin (0.1–0.9 μ g) inhibited mechanical allodynia in neuropathic pain models induced by chemotherapy¹⁰. Intraplantar injection of QX-314 (2%, approximately 60 mM; 10 μ L) and capsaicin (1 μ g/ μ L; 10 μ L) together produced long-lasting increase in mechanical and thermal nociceptive thresholds¹¹. We first examined whether sensory fiber-specific silencing in vivo affected the responses of sensory afferent fibers by using transcutaneous sine wave stimuli in wild-type mice. Transcutaneous nerve stimulation was conducted using three sine wave pulses with frequencies of 5, 250, and 2000 Hz to activate the C, A δ , and A β fibers, respectively^{12, 13}. As shown in Fig. 1, when 20 μ L of QX-314 (30 mM) with flagellin (0.5 μ g in 20 μ L) were simultaneously injected into the subcutaneous plantar hind paw of wild-type mice, the paw withdrawal threshold to stimuli at frequencies of 250 Hz and 2000 Hz, but not 5 Hz, were significantly increased at 1 h after the injection compared to the vehicle-treated mice (Fig. 1b, 250 Hz: vehicle: 430 \pm 44 μ A (n = 9) vs. QX-314 + flagellin: 654 \pm 61 μ A (n = 9), $P = 0.0005$; Fig. 1c, 2000 Hz: vehicle: 604 \pm 47 μ A vs. QX-314 + flagellin: 789 \pm 55 μ A, $P = 0.0406$). Intraplantar co-injection of QX-314 (30 mM) and capsaicin (10 μ g in 20 μ L) increased the paw withdrawal threshold to stimuli at frequencies of 5 Hz, but not at 250 Hz and 2000 Hz, in wild-type mice (Fig. 1a, 1 h, vehicle: 444 \pm 49 μ A (n = 9)

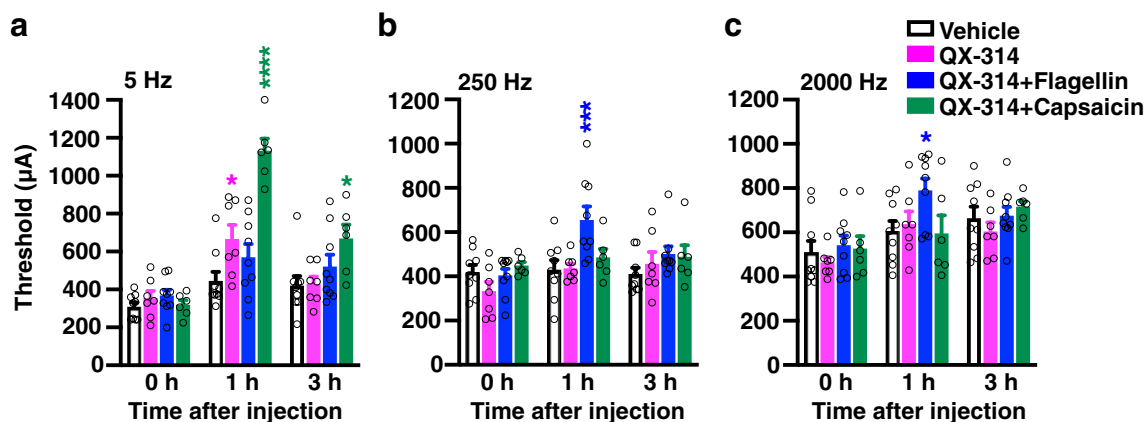


Figure 1. Effect of pharmacological sensory fiber-specific silencing on the responses of sensory afferent fibers using transcutaneous sine wave stimuli in *Tnxb*^{+/+} mice. The current threshold represents the minimum intensity (μ A) required to produce a paw withdrawal response with sine wave electrical stimulation at 5 Hz (a), 250 Hz (b), and 2000 Hz (c) in mice at the indicated time after intraplantar (i.pl.) administration of vehicle, QX-314 (30 mM), QX-314 (30 mM) plus flagellin (0.5 μ g) for A-fiber silencing, and QX-314 (30 mM) plus capsaicin (10 μ g) for C-fiber silencing. Vehicle (n = 9), QX-314 (n = 7), QX-314 + flagellin (n = 9), and QX-314 + capsaicin (n = 6). **** $P < 0.0001$, *** $P < 0.001$, * $P < 0.05$ versus the vehicle-treated value, two-way repeated measurement ANOVA revealed a significant treatment (5 Hz: $F_{(3,27)} = 18.44$, $P < 0.0001$; 250 Hz: $F_{(3,27)} = 3.266$, $P = 0.0366$; 2000 Hz: $F_{(3,27)} = 3.118$, $P = 0.0425$) with post hoc Bonferroni's multiple comparison test. The data are expressed as the mean \pm S.E.M.

vs. QX-314 + capsaicin: $1131 \pm 65 \mu\text{A}$ ($n=6$), $P < 0.0001$; 3 h, vehicle: $420 \pm 52 \mu\text{A}$ vs. QX-314 + capsaicin: $669 \pm 73 \mu\text{A}$, $P = 0.0127$). Intraplantar administration of QX-314 (30 mM) alone slightly increased the paw withdrawal threshold to stimuli at frequencies of 5 Hz (1 h, vehicle: $444 \pm 49 \mu\text{A}$ ($n=9$) vs. QX-314: $666 \pm 75 \mu\text{A}$ ($n=7$), $P = 0.0245$); however, the increase in the paw withdrawal threshold induced by QX-314 alone was much lower than that induced by QX-314 plus capsaicin (Fig. 1a). These results suggested that co-injection of QX-314 and flagellin leads to silencing of A δ (250 Hz) and A β (2000 Hz) fibers, while co-injection of QX-314 and capsaicin silences C fibers (5 Hz) in the wild-type mice.

Sensory A-fiber silencing in vivo on the mechanical allodynia and the central sensitization in *Tnxb*^{-/-} mice

We examined whether sensory A-fiber silencing in vivo affected the mechanical allodynia in *Tnxb*^{-/-} mice. *Tnxb*^{-/-} mice significantly decreased in 50% paw withdrawal threshold to von Frey filaments, leading to mechanical allodynia, compared to wild-type mice (Fig. 2a, *Tnxb*^{+/+}: 1.22 ± 0.15 g ($n=13$) vs. *Tnxb*^{-/-}: 0.26 ± 0.03 g ($n=30$), $P < 0.0001$), as with previous our report⁹. Intraplantar co-injection (20 μL) of QX-314 (30 mM) with flagellin (0.5 μg) significantly increased the 50% paw withdrawal threshold at 0.5 h and 1 h after the injection in *Tnxb*^{-/-} mice, compared to the vehicle-treated mice (Fig. 2b, 0.5 h, vehicle: 0.19 ± 0.06 g ($n=8$) vs. QX-314 + flagellin: 0.84 ± 0.23 g ($n=7$), $P = 0.0108$; 1 h, vehicle: 0.12 ± 0.03 g vs. QX-314 + flagellin: 1.02 ± 0.22 g, $P = 0.0001$). This increase in the paw withdrawal threshold induced by QX-314 plus flagellin returned to the pre-administration level at 6 h in *Tnxb*^{-/-} mice. These results indicated that A fiber silencing, intraplantar injections of QX-314 plus flagellin, suppressed the mechanical allodynia in *Tnxb*^{-/-} mice.

Furthermore, we examined the effect of A-fiber silencing on the central sensitization in the spinal dorsal horn of *Tnxb*^{-/-} mice. Both the neuronal activation marker c-Fos and the nociceptive-specific activation marker phosphorylated extracellular signal-regulated kinase (p-ERK) in spinal cord are induced by noxious stimuli via C- and A δ -fibers^{14–16}, and by A β -fiber activation following nerve injury¹⁷. c-Fos is also activated by innocuous stimuli via A β fiber^{14, 18}. In this study, we performed immunostaining of spinal dorsal horn by using c-Fos antibody to clarify the effect of A-fiber silencing. As shown in Fig. 3, the numbers of c-Fos-immunoreactive neurons significantly increased in laminae I and II and in laminae III–V of the spinal dorsal horn in *Tnxb*^{-/-} mice injected with vehicle, as compared to *Tnxb*^{+/+} mice (laminae I, II, *Tnxb*^{+/+}: 3.79 ± 3.02 ($n=3$) vs. *Tnxb*^{-/-} with vehicle: 73.3 ± 10.6 ($n=3$), $P = 0.0279$; laminae III–V, *Tnxb*^{+/+}: 25.1 ± 2.62 ($n=3$) vs. *Tnxb*^{-/-} with vehicle: 41.9 ± 1.24 ($n=3$), $P = 0.0215$). When QX-314 (30 mM) plus flagellin (0.5 μg) were injected into the subcutaneous of plantar hind paw in *Tnxb*^{-/-} mice, numbers of c-Fos-immunoreactive neurons significantly decreased in laminae I and II and in laminae III–V of ipsilateral spinal dorsal horn at 1 h after the injection, as compared to those of *Tnxb*^{-/-} mice injected with vehicle (laminae I, II, *Tnxb*^{-/-} with vehicle: 73.3 ± 10.6 ($n=3$) vs. *Tnxb*^{-/-} with QX-314 + flagellin: 37.7 ± 5.09 ($n=3$), $P = 0.0272$ ($n=14$), $P < 0.0001$; laminae III–V, *Tnxb*^{-/-} with vehicle: 41.9 ± 3.20 ($n=15$) vs. *Tnxb*^{-/-} with QX-314 + flagellin: 26.2 ± 4.61 ($n=3$), $P = 0.0290$). These results indicated that A-fiber silencing, intraplantar injections of QX-314 plus flagellin, blocked the central sensitization in the spinal dorsal horn of *Tnxb*^{-/-} mice.

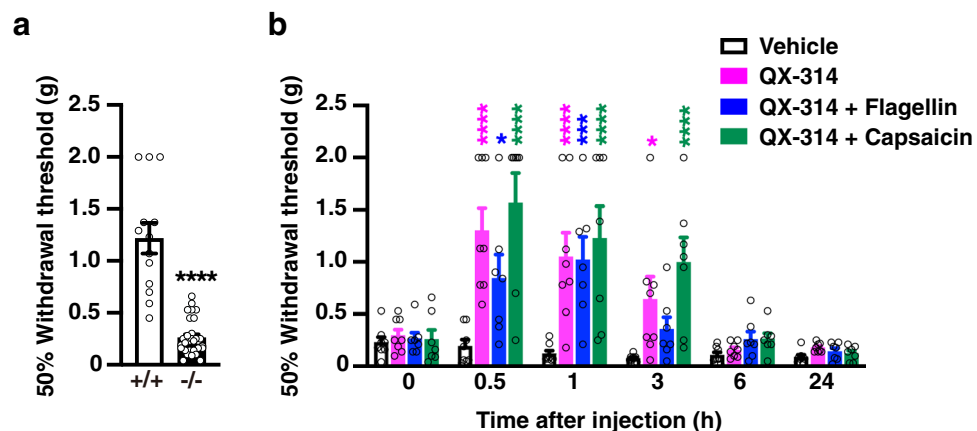


Figure 2. Effect of pharmacological sensory fiber-specific silencing on the mechanical allodynia in *Tnxb*^{-/-} mice. **(a)** Mechanical allodynia in *Tnxb*^{-/-} mice. 50% paw withdrawal threshold to von Frey filaments was measured in *Tnxb*^{+/+} mice ($n=13$) and *Tnxb*^{-/-} mice ($n=30$). **** $P < 0.0001$ versus *Tnxb*^{+/+} mice, unpaired t test $t_{41} = 8.952$. **(b)** Effects of i.pl. QX-314 (30 mM), QX-314 (30 mM) plus flagellin (0.5 μg), and QX-314 (30 mM) plus capsaicin (10 μg) on the mechanical allodynia in *Tnxb*^{-/-} mice. 50% paw withdrawal thresholds to von Frey filaments were assessed in *Tnxb*^{-/-} mice by i.pl. administration of vehicle ($n=8$), QX-314 ($n=8$), QX-314 + flagellin ($n=7$), or QX-314 + capsaicin ($n=7$). **** $P < 0.0001$, *** $P < 0.001$, * $P < 0.05$ versus the vehicle-treated value, two-way repeated measurement ANOVA revealed significant time \times treatment interaction ($F_{(15,130)} = 4.233$, $P < 0.0001$) and treatment ($F_{(3,26)} = 11.34$, $P < 0.0001$) with post hoc Bonferroni's multiple comparison test. The data are expressed as the mean \pm S.E.M.

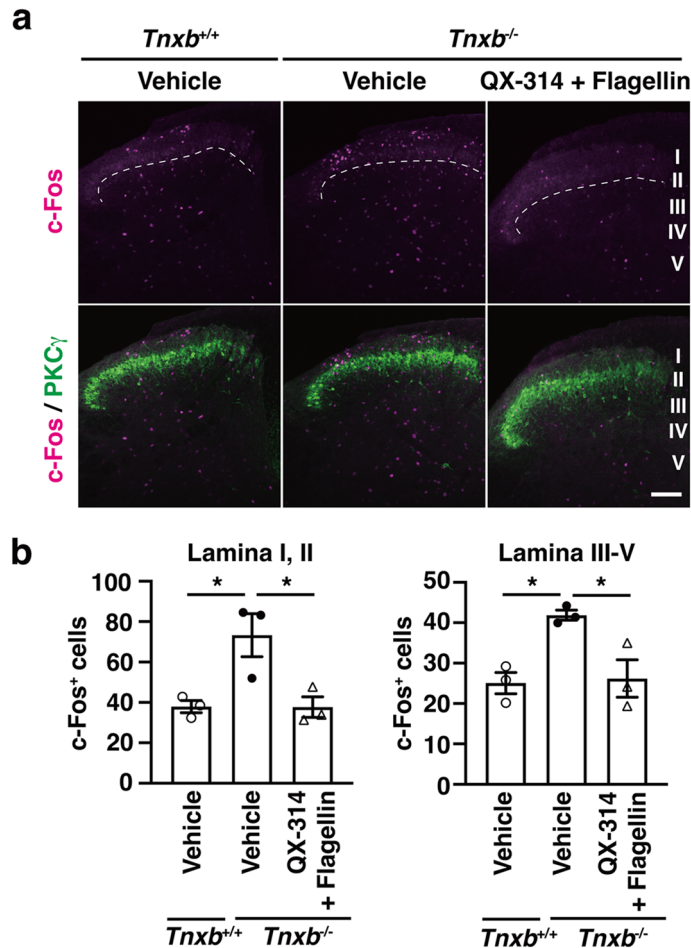


Figure 3. Effect of pharmacological A-fiber silencing on the central sensitization in the spinal dorsal horns of *Tnxb*^{-/-} mice. **(a)** Representative fluorescence images of c-Fos (magenta) and PKC γ (green) immunoreactivity in the spinal dorsal horn of *Tnxb*^{+/+} and *Tnxb*^{-/-} mice injected i.pl. with vehicle or QX-314 (30 mM) + flagellin (0.5 μ g). PKC γ was used as a marker of lamina III. The dotted lines show the border between lamina II and lamina III. Scale bar, 100 μ m. **(b)** The numbers of c-Fos⁺ cells in laminae I, II and III-V of the spinal dorsal horn ($n = 3$ mice, 4–5 sections per mouse). * $P < 0.05$, one-way ANOVA revealed laminae I, II ($F_{(2,6)} = 8.469$, $P = 0.0179$) and laminae III-V ($F_{(2,6)} = 8.909$, $P = 0.0160$) with post hoc Tukey's multiple comparison test. The data are expressed as the mean \pm S.E.M.

Sensory C-fiber silencing in vivo on the mechanical allodynia in *Tnxb*^{-/-} mice

To characterize the specificity of A-fiber silencing on mechanical allodynia in *Tnxb*^{-/-} mice, we determined whether C-fiber silencing by co-injection of QX-314 and capsaicin affects mechanical allodynia in *Tnxb*^{-/-} mice. Significant increases in the 50% paw withdrawal threshold were observed following intraplantar injection (20 μ L) of QX-314 (30 mM) plus capsaicin (10 μ g) or QX-314 (30 mM) alone in *Tnxb*^{-/-} mice. Intraplantar injection of QX-314 plus capsaicin significantly increased the paw withdrawal threshold from 0.5 to 3 h after the application in *Tnxb*^{-/-} mice compared to vehicle-treated mice (Fig. 2b, 0.5 h, vehicle: 0.19 ± 0.06 g ($n = 8$) vs. QX-314 + capsaicin ($n = 7$): 1.56 ± 0.29 g, $P < 0.0001$; 1 h, vehicle: 0.12 ± 0.03 g vs. QX-314 + capsaicin: 1.23 ± 0.31 g, $P < 0.0001$; 3 h, vehicle: 0.08 ± 0.01 g vs. QX-314 + capsaicin: 1.00 ± 0.24 g, $P < 0.0001$). Intraplantar injection of QX-314 alone also increased the paw withdrawal threshold at 0.5 h and 1 h after the application in *Tnxb*^{-/-} mice compared to vehicle-treated mice (Fig. 2b, 0.5 h, vehicle: 0.19 ± 0.06 g ($n = 8$) vs. QX-314 ($n = 8$): 1.30 ± 0.21 g, $P < 0.0001$; 1 h, vehicle: 0.12 ± 0.03 g vs. QX-314: 1.05 ± 0.23 g, $P < 0.0001$). Taken together, there is no significant difference in the increases of paw withdrawal threshold among QX-314 alone, QX-314 plus flagellin, and QX-314 plus capsaicin (Fig. 2b). These results indicated that QX-314 alone inhibited the mechanical allodynia in *Tnxb*^{-/-} mice.

Effects of sensory fiber silencing in vivo and QX-314 alone on the responses of sensory afferent fibers in *Tnxb*^{-/-} mice

We further examined whether sensory fiber silencing in vivo and QX-314 alone affected the responses of sensory afferent fibers by using transcutaneous sine wave stimuli in *Tnxb*^{-/-} mice. Similarly to our previous findings⁹, the paw threshold for the 250- and 2000-Hz stimulus responses were significantly reduced in *Tnxb*^{-/-} mice compared with those in wild-type mice before the administration of drugs (Table 1, 250 Hz, wild-type: 401 ± 17 μ A

| | | Threshold (μA) | | |
|----------------------------|----------|-----------------------------|------------------|---------------|
| | | 5 Hz | 250 Hz | 2000 Hz |
| <i>Tnxb</i> ^{+/+} | (n = 31) | 337 \pm 15 | 401 \pm 17 | 511 \pm 23 |
| <i>Tnxb</i> ^{-/-} | (n = 40) | 302 \pm 13 | 288 \pm 16**** | 438 \pm 19* |

Table 1. Paw withdrawal thresholds in responses to sine-wave electrical stimuli in *Tnxb*^{+/+} and *Tnxb*^{-/-} mice before the administration of drugs. The current threshold represents the minimum intensity (μA) required to produce a paw withdrawal response with sine wave electrical stimulation at 5, 250, and 2000 Hz. The data **** $P < 0.0001$, * $P < 0.05$ versus the *Tnxb*^{+/+} value, unpaired *t* test 5 Hz: $t_{69} = 1.744$, 250 Hz: $t_{69} = 4.672$, 2000 Hz: $t_{69} = 2.460$. The data are expressed as the mean \pm S.E.M. from experiments using *Tnxb*^{+/+} (Fig. 1) and *Tnxb*^{-/-} mice (Fig. 4).

(n = 31) vs. *Tnxb*^{-/-}: 288 \pm 16 μA (n = 40), $P < 0.0001$; 2000 Hz, wild-type: 511 \pm 23 μA vs. *Tnxb*^{-/-}: 438 \pm 19 μA , $P = 0.0164$). As shown in Fig. 4b,c, intraplantar administration of QX-314 plus flagellin significantly increased the threshold at frequencies of 250 Hz and 2000 Hz in *Tnxb*^{-/-} mice, compared to vehicle administration (250 Hz: 1 h, vehicle: 259 \pm 28 μA (n = 6) vs. QX-314 + flagellin: 432 \pm 36 μA (n = 13), $P = 0.0119$; 3 h, vehicle: 216 \pm 9.7 μA vs. QX-314 + flagellin: 429 \pm 30 μA , $P = 0.0009$; 2000 Hz: 3 h, vehicle: 400 \pm 20 μA vs. QX-314 + flagellin: 690 \pm 42 μA , $P = 0.0024$). Intraplantar administration of QX-314 plus capsaicin also increased the paw withdrawal threshold in the stimuli at frequencies of 250 Hz and 2000 Hz in *Tnxb*^{-/-} mice (250 Hz: 1 h, vehicle: 259 \pm 28 μA (n = 6) vs. QX-314 + capsaicin: 478 \pm 36 μA (n = 10), $P = 0.0012$; 2000 Hz: 3 h, vehicle: 400 \pm 20 μA vs. QX-314 + capsaicin: 717 \pm 63 μA , $P = 0.0013$), different from that of wild-type mice (Fig. 1b,c). Furthermore, the threshold level induced by the co-application of QX-314 with flagellin or capsaicin was similar to that induced by QX-314 alone in the stimuli at frequencies of 250 Hz and 2000 Hz in *Tnxb*^{-/-} mice. The QX-314 alone-induced threshold increase was approximately 1.6–1.8-fold higher than the vehicle-induced one in 1 h and 3 h after the administration at frequencies of 250 Hz (1 h, vehicle: 259 \pm 28 μA (n = 6) vs. QX-314: 430 \pm 64 μA (n = 11), $P = 0.0172$, 3 h, vehicle: 216 \pm 9.8 μA vs. QX-314: 378 \pm 40 μA , $P = 0.0272$) and in 3-h at frequencies of 2000 Hz (vehicle: 400 \pm 20 μA vs. QX-314: 620 \pm 69 μA , $P = 0.0497$) in *Tnxb*^{-/-} mice. Consistent with the results of paw withdrawal threshold, QX-314 alone, QX-314 plus flagellin, and QX-314 plus capsaicin affected the thresholds for A-fibers responded by the 250- and 2000-Hz stimulus in *Tnxb*^{-/-} mice.

In the response to transcutaneous sine wave stimuli at a frequency of 5 Hz, there was no significant difference between wild-type and *Tnxb*^{-/-} mice before the administration of drugs (Table 1, wild-type: 337 \pm 15 μA (n = 31) vs. *Tnxb*^{-/-}: 302 \pm 13 μA (n = 40), $P = 0.0857$). Intraplantar administration of QX-314 plus capsaicin significantly increased at 1 h and 3 h compared to vehicle administration in *Tnxb*^{-/-} mice (Fig. 4a, 1 h, vehicle: 323 \pm 26 μA (n = 6) vs. QX-314 + capsaicin: 624 \pm 36 μA (n = 10), $P = 0.0007$, 3 h, vehicle: 280 \pm 35 μA vs. QX-314 + capsaicin: 615 \pm 56 μA , $P = 0.0001$); however, the maximum increase observed at 1 h in *Tnxb*^{-/-} mice was substantially lower than that in wild-type mice (Fig. 1a). This result suggests that the TNX deficiency affects the C-fiber silencing mechanisms induced by QX-314 plus capsaicin. Furthermore, intraplantar administration of QX-314 plus flagellin, but not QX-314 alone, increased the threshold at frequencies of 5 Hz, in addition to frequencies

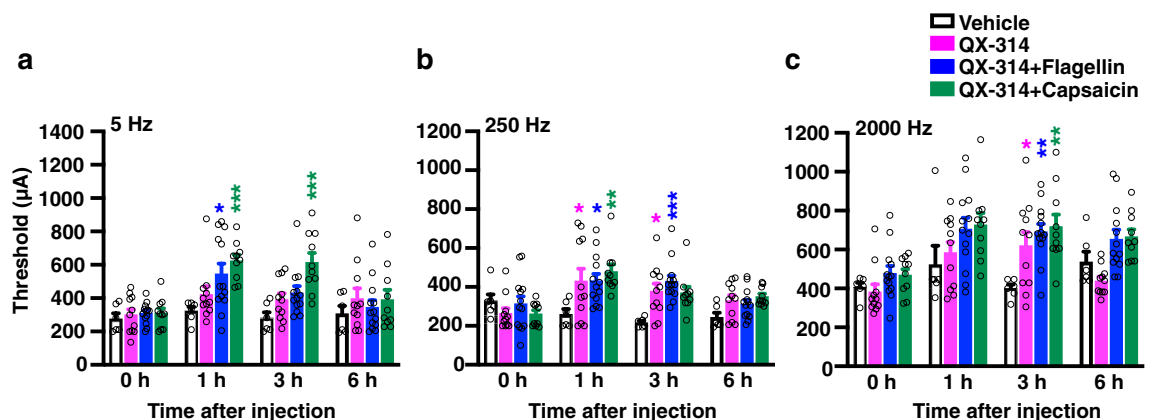


Figure 4. Effects of pharmacological sensory fiber-specific silencing on the responses of sensory afferent fibers using transcutaneous sine wave stimuli in *Tnxb*^{-/-} mice. The current threshold represents the minimum intensity (μA) required to produce a paw withdrawal response with sine wave electrical stimulation at 5 Hz (a), 250 Hz (b), and 2000 Hz (c) in mice at the indicated time after i.pl. administration of vehicle, QX-314 (30 mM) plus flagellin (0.5 μg), and QX-314 (30 mM) plus capsaicin (10 μg). Vehicle (n = 6), QX-314 (n = 11), QX-314 + flagellin (n = 13), and QX-314 + capsaicin (n = 10). **** $P < 0.001$, ** $P < 0.01$, * $P < 0.05$ versus the vehicle-treated value, two-way repeated measurement ANOVA revealed a significant treatment (5 Hz: $F_{(3,36)} = 7.007$, $P = 0.0008$; 250 Hz: $F_{(3,36)} = 4.872$, $P = 0.0060$; 2000 Hz: $F_{(3,36)} = 6.524$, $P = 0.0012$) with post hoc Bonferroni's multiple comparison test. The data are expressed as the mean \pm S.E.M.

of 250 Hz and 2000 Hz, in *Tnxb^{-/-}* mice (Fig. 4a, 1 h, vehicle: $323 \pm 26 \mu\text{A}$ ($n=6$) vs. QX-314 + flagellin: $544 \pm 62 \mu\text{A}$ ($n=13$), $P=0.0160$), indicating that administration of QX-314 plus flagellin also affects the C-fiber response in *Tnxb^{-/-}* mice.

QX-314-induced inhibition of mechanical allodynia through TLR5-dependent activation in *Tnxb^{-/-}* mice

Intraplantar co-injection of QX-314 with flagellin, but not QX-314 alone, increased the paw withdrawal thresholds of A β - and A δ -fibers in wild-type mice (Fig. 1b,c). On the other hand, intraplantar injection of QX-314 alone led to the increase of thresholds responded for A β - and A δ -fibers (Fig. 4b,c) and inhibition of mechanical allodynia (Fig. 2b) in *Tnxb^{-/-}* mice. Therefore, we hypothesized that the effects of QX-314 alone are mediated by constitutive activation of TLR5 in *Tnxb^{-/-}* mice. To investigate this possibility, we examined the effect of a potent and selective TLR5/flagellin complex antagonist, TH1020, on mechanical allodynia in *Tnxb^{-/-}* mice. Pre-administration of TH1020 markedly suppressed the QX-314-induced increase of 50% paw withdrawal threshold (Fig. 5a), and the significant decrease induced by TH1020 was observed at 0.5 h after the injection of QX-314 (vehicle pre-injection + QX-314: $1.50 \pm 0.26 \text{ g}$ ($n=7$) vs. TH1020 pre-injection + QX-314: $0.59 \pm 0.26 \text{ g}$ ($n=8$), $P=0.0033$). Intraplantar injection of TH1020 (10 nmol, 4.5 μg) did not affect the TNX-deficiency-induced

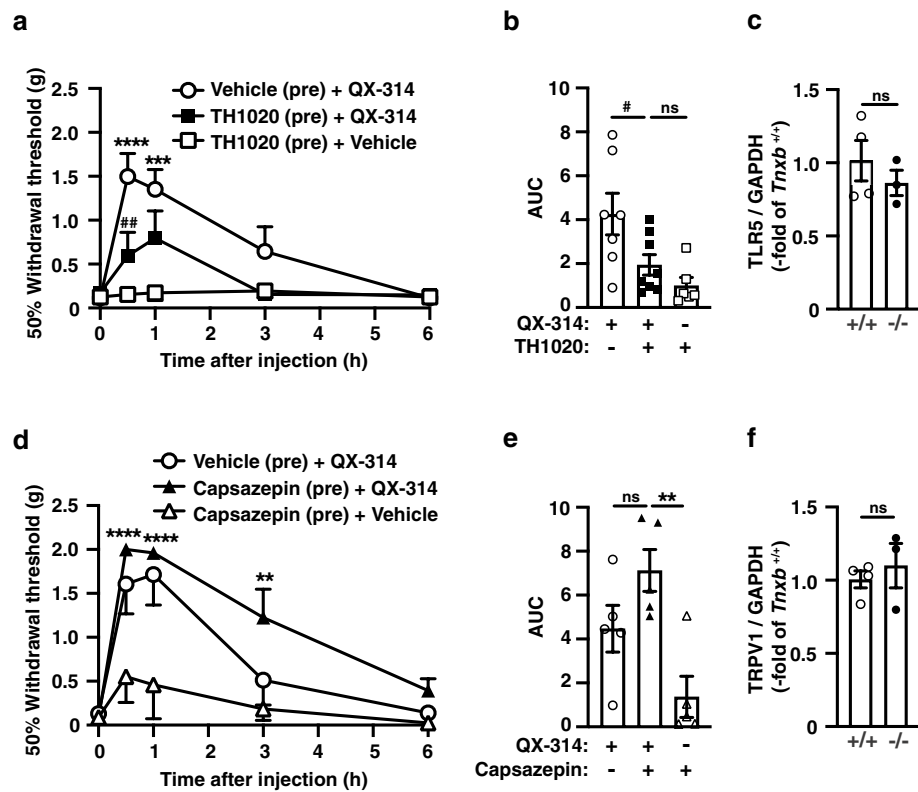


Figure 5. Blocking of the QX-314-induced inhibition of mechanical allodynia by a TLR5/flagellin complex antagonist TH1020 in *Tnxb^{-/-}* mice. (a) TH1020 (10 nmol, 4.5 μg) or vehicle was intraplantar administrated at 30-min before QX-314 (60 mM; 10 μL) injection in *Tnxb^{-/-}* mice. 50% paw withdrawal thresholds to von Frey filaments were assessed in *Tnxb^{-/-}* mice by i.p. administration of TH1020 ($n=6$), vehicle(pre) + QX-314 ($n=7$), or TH1020 + QX-314 ($n=8$). $^{##}P < 0.01$ versus the vehicle(pre) + QX-314 treated value, $^{****}P < 0.0001$, $^{***}P < 0.001$ versus the TH1020(pre) + vehicle treated value, two-way repeated measurement ANOVA revealed significant time \times treatment interaction ($F_{(8,72)} = 4.712$, $P = 0.0001$) and treatment ($F_{(2,18)} = 7.321$, $P = 0.0047$) with post hoc Bonferroni's multiple comparison test. (b) AUC based on data from (a) were represented. $^{**}P < 0.01$, $^{*}P < 0.05$, one-way ANOVA ($F_{(2,18)} = 6.257$, $P = 0.0086$) with post hoc Tukey's multiple comparison test. (c) Expression of TLR5 mRNA in dorsal root ganglion of wild-type and *Tnxb^{-/-}* mice. (d) A TRPV1 antagonist capsazepine (27 nmol, 10 μg) or vehicle was intraplantar administrated at 30-min before QX-314 (60 mM; 10 μL) injection in *Tnxb^{-/-}* mice. 50% paw withdrawal thresholds to von Frey filaments were assessed in *Tnxb^{-/-}* mice by i.p. administration of capsazepine(pre) + vehicle ($n=5$), vehicle(pre) + QX-314 ($n=5$), or capsazepine(pre) + QX-314 ($n=5$). $^{****}P < 0.0001$, $^{***}P < 0.001$, $^{**}P < 0.01$ versus the capsazepine(pre) + vehicle treated value, two-way repeated measurement ANOVA revealed significant time \times treatment interaction ($F_{(8,48)} = 4.156$, $P = 0.0008$) and treatment ($F_{(2,12)} = 9.906$, $P = 0.0029$) with post hoc Bonferroni's multiple comparison test. (e) AUC based on data from (d) were represented. $^{**}P < 0.01$, $^{*}P < 0.05$, one-way ANOVA ($F_{(2,12)} = 8.535$, $P = 0.0049$) with post hoc Tukey's multiple comparison test. (f) Expression of TRPV1 mRNA in dorsal root ganglion of wild-type and *Tnxb^{-/-}* mice. The data are expressed as the mean \pm S.E.M.

mechanical allodynia. Area under the curve (AUC) of 50% paw withdrawal threshold induced by QX-314 alone was also inhibited by pre-administration of TH1020 in *Tnxb*^{-/-} mice (Fig. 5b). In contrast to TH1020, pre-administration of 10 nmol (4.5 µg) capsazepine, a TRPV1 antagonist, had no significant effect on QX-314-induced inhibition of mechanical allodynia in *Tnxb*^{-/-} mice (Fig. 5d,e). We analyzed the expression of TLR5 and TRPV1 mRNAs in dorsal root ganglion, which contained some of sensory neurons, of *Tnxb*^{-/-} mice. There is no significant difference in mRNA expression of TLR5 and TRPV1 between wild-type and *Tnxb*^{-/-} mice (Fig. 5c and f). These results indicated that inhibition of mechanical allodynia with QX-314 alone is mediated by constitutive activation of TLR5 in *Tnxb*^{-/-} mice.

Discussion

In the present study, we revealed that the mechanical allodynia and central sensitization of the spinal dorsal horn were mediated by the hypersensitization of Aβ and Aδ fibers in *Tnxb*^{-/-} mice, by using pharmacological sensory fiber silencing. A-fiber silencing, intraplantar (i.pl.) co-administration of QX-314 and flagellin, significantly increased the paw withdrawal threshold of Aβ and Aδ fibers to transcutaneous sine wave stimuli at frequencies of 250 Hz and 2000 Hz, respectively, in wild-type mice. Intraplantar co-administration of QX-314 and flagellin significantly increased the paw withdrawal threshold of Aβ and Aδ fibers in *Tnxb*^{-/-} mice, and it inhibited the mechanical allodynia and spinal neuronal activation in *Tnxb*^{-/-} mice. Notably, in *Tnxb*^{-/-} mice, but not wild-type mice, i.pl. administration of QX-314 alone significantly increased the paw withdrawal threshold of Aβ and Aδ fibers and subsequent mechanical allodynia. Thus, the activation of Aβ and Aδ fibers led to the TNX deficiency induced-mechanical allodynia. Furthermore, the QX-314-induced inhibition of mechanical allodynia was reduced by TLR5 antagonist TH1020, suggesting that it is mediated via constitutive activation of TLR5.

Blocking A-fibers can be specifically achieved by using TLR5 ligand flagellin and the membrane-impermeable sodium channel blocker QX-314¹⁰. Likewise, i.pl. co-administration of QX-314 and flagellin significantly increased the paw withdrawal threshold of Aβ and Aδ fibers to transcutaneous sine wave stimuli at frequencies of 250 Hz and 2000 Hz in wild-type mice (Fig. 1). The QX-314 plus flagellin-induced increase of threshold to stimuli at frequencies of 250 Hz and 2000 Hz was also observed in *Tnxb*^{-/-} mice (Fig. 4). We have previously reported that TNX deficiency induces mechanical allodynia and central sensitization in the dorsal horn of the spinal cord, in addition to hypersensitization of myelinated Aβ and Aδ fibers⁹. A-fiber silencing, i.pl. co-administration of QX-314 and flagellin, significantly inhibited the mechanical allodynia (Fig. 2) and the increase of c-Fos positive neurons of spinal dorsal horn (Fig. 3). Surprisingly, intraplantar administration of QX-314 alone significantly increased the paw withdrawal threshold to stimuli at frequencies of 250 Hz and 2000 Hz in *Tnxb*^{-/-} mice (Fig. 4) but not wild-type mice (Fig. 1). Intraplantar administration of QX-314 alone inhibited the mechanical allodynia in *Tnxb*^{-/-} mice (Fig. 2). These results suggest that hypersensitization of myelinated Aβ and Aδ fibers responded to stimuli at frequencies of 250 Hz and 2000 Hz led to the mechanical allodynia.

QX-314 is a membrane-impermeable voltage-gated sodium channels blocker that blocks these channels by binding to their intracellular domains. Although the extracellular application of QX-314 theoretically has no effect on the activity of sodium channels, QX-314 has been shown to enter the cytoplasm of cells by activating the TRPV1 channel¹¹. Intraplantar co-administration of QX-314 (2% (approximately 60 mM), 10 µL) and capsaicin (1 µg/µL, 10 µL) increased the mechanical threshold for paw withdrawal using von Frey filaments, whereas i.pl. administration of QX-314 alone had no significant effect on the mechanical threshold. In this study, i.pl. administration of QX-314 (30 mM) without a TRPV1 agonist inhibited mechanical allodynia in *Tnxb*^{-/-} mice (Fig. 2b). Consistent with this result, QX-314 (2%, 60 mM) alone applied i.pl. to UV-burn-induced inflamed paws has an inhibitory effect on paw mechanical sensitivity¹⁹. During tissue damage and inflammation, inflammatory mediators such as ATP, prostaglandins, and bradykinin released from surrounding damaged or inflamed tissues and the acidic environment surrounding the inflamed tissues have been reported to sensitize the response of TRPV1^{20,21}. Furthermore, systemic intraperitoneal administration of QX-314 (1–3 mg/kg) alone reduced bone cancer pain-related behaviors by inhibiting TRPV1-expressing afferents²². In a bone cancer pain model, tumor growth induces inflammation and an acidic environment is induced by activated osteoclasts²³. These reports suggest that the inhibitory effects of QX-314 alone are mediated by TRPV1 activation. However, the TRPV1 antagonist capsazepine failed to suppress the inhibition of mechanical allodynia induced by i.pl. administration of QX-314 alone in *Tnxb*^{-/-} mice (Figs. 5d,e), suggesting that the inhibitory mechanisms of QX-314 alone are independent of TRPV1 channel activation. We identified a novel mechanism of action for i.pl. QX-314 alone, in which TLR5 was involved in inhibiting mechanical allodynia in *Tnxb*^{-/-} mice. A potent and selective TLR5/flagellin complex antagonist, TH1020, blocked the QX-314-induced inhibition of mechanical allodynia in *Tnxb*^{-/-} mice (Figs. 5a,b). Flagellin, a TLR5 agonist, induces the entry of extracellular QX-314 into the cytoplasm via unidentified pores such as channel¹⁰. Thus, TNX-deficiency may lead to constitutive activation of TLR5 and subsequent cellular signaling.

Axonal polyneuropathy occurs in TNX-deficient EDS patients^{3,5,24}. Nerve conduction studies were abnormal in 80% of TNX-deficient EDS patients, and fulfilled the criteria of sensorimotor axonal polyneuropathy in 40% of the patients⁵. Electromyography shows TNX-deficient EDS patients had a predominant neurogenic and a mixed myogenic-neurogenic patterns⁵. Neuropathic symptoms including paresthesia are frequently observed in patients with TNX-deficient EDS^{3,5}. Voermans et al. reported histological changes in sciatic nerves such as mildly smaller inner and outer diameters of the myelinated fiber and reduced collagen fibril density of the endoneurium in *Tnxb*^{-/-} mice²⁵. We have reported that TNX deficiency induces hypersensitivity of myelinated Aβ and Aδ fibers, whereas it has no effect on C-fiber response under the basal condition⁹. In this study, A-fiber silencing, co-administration of QX-314 and flagellin, affected the paw withdrawal threshold of C fiber to stimuli at frequencies of 5 Hz in *Tnxb*^{-/-} mice (Fig. 4a). This finding raises a possibility that A fibers partially cross over C fiber in sensory fibers of *Tnxb*^{-/-} mice. Fiber interaction such as ephaptic and cross-excitation is thought to

be one of peripheral neuropathy mechanisms whereby nociceptive fibers such as C- and A δ -fibers could be stimulated by activity in low-threshold mechanoreceptors in non-nociceptive A β fibers^{26–29}. TNX-deficiency may induce physical crosstalk between A fibers and C fibers. In addition, C-fiber silencing effect of the paw withdrawal threshold for responses to 5 Hz stimuli in *Tnxb*^{-/-} mice was lower than that in wild-type mice, although administration of QX-314 plus capsaicin significantly increased the threshold at a frequency of 5 Hz in both wild-type and *Tnxb*^{-/-} mice (Figs. 1a and 4a). There was no difference in the threshold for responses to 5 Hz stimuli at pre-administration between wild-type and *Tnxb*^{-/-} mice. These results suggest that TNX deficiency affects the C-fiber silencing mechanisms by using QX-314 and capsaicin. The expression level of the capsaicin receptor TRPV1 mRNA in dorsal root ganglion of *Tnxb*^{-/-} mice was similar to that of wild-type mice (Fig. 5f). TNX-deficient mice showed normal behavioral response to the noxious thermal stimulation in hot plate-test⁹, whereas TRPV1-deficient mice showed impaired behavioral response to the noxious thermal stimulation compared to wild-type mice³⁰. Taken together, TNX deficiency inhibits the QX-314 plus capsaicin-evoked C-fiber silencing through an undetermined mechanism independent of TRPV1. The pathophysiological mechanism of peripheral neuropathy in patients with TNX-deficient EDS seems to be related to the dysfunction of unmyelinated C-fibers, in addition to the hypersensitivity of myelinated A β and A δ fibers.

In conclusions, we demonstrated that the TNX deficiency-induced mechanical allodynia is mediated by A-fiber hypersensitivity using pharmacological sensory fiber silencing with co-administration of QX-314 and flagellin. In addition, QX-314 alone led to the silencing of A-fiber responses and inhibition of mechanical allodynia through the constitutive activation of TLR5 in *Tnxb*^{-/-} mice. Our findings will be useful for managing neurological complications in patients with EDS.

Methods

Animals

All experiments were approved by the Animal Experimentation Committee of the Osaka Institute of Technology and were performed in accordance with the National Institutes of Health Guide for the Care and Use of Laboratory Animals and the ethical guidelines of the Ethics Committee of the International Association for the Study of Pain. This study was conducted in accordance with ARRIVE guidelines. *Tnxb*^{-/-} mice were generated as previously reported³¹, and they were backcrossed with C57BL/6 J mice for ten generations. Age-matched C57BL/6 J mice were used as wild-type (*Tnxb*^{+/+}) mice. Seven to 9-week-old male mice were used for the experiments, because of the marked sex-related differences in mechanisms of pain hypersensitivity³². Animals were housed under conditions of a 12-h light/12-h dark cycle and at a constant temperature of 22 \pm 2 °C. Animals were allowed free access to food and water prior to testing.

Administration of drug and antibody

Capsaicin and capsazepine were purchased from Fujifilm Wako Pure Chemical (Osaka, Japan), flagellin from Sigma-Aldrich (St. Louis, MO, USA), QX-314 from Abcam (Cambridge, UK), and TH1020 from MedChemExpress (Monmouth Junction, NJ, USA). Capsaicin (1 mg/mL) was dissolved in saline containing 20% ethanol and 5% Tween 20. Flagellin (0.1 mg/mL) was dissolved in distilled water, TH1020 (8.8 mM, 4 mg/mL) was dissolved in dimethyl sulfoxide and diluted to a final concentration with saline. QX-314 was dissolved in a saline solution. Capsazepine (1 mg/mL) was dissolved in saline containing 5% dimethyl sulfoxide and 5% Tween 20. Mice were injected subcutaneously into the plantar surface of the hind paw with 20 μ L of QX-314 (30 mM), QX-314 (30 mM) plus flagellin (0.5 μ g in 20 μ L), QX-314 (30 mM) plus capsaicin (10 μ g in 20 μ L), and TH1020 (10 nmol, 4.5 μ g), using 27-gauge stainless steel needle attached to a microsyringe. For pre-administration of TH1020 or capsazepine, mice were subcutaneously injected with 10 μ L of TH1020 (10 nmol in 10 μ L), capsazepine (10 μ g in 10 μ L), or vehicle, and then 10 μ L of QX-314 (60 mM) was administered 30 min after administration. All drug administration experiments were performed by investigators blinded to the drugs.

von Frey test

Mice were randomly placed in glass chambers on a mesh floor. Mice were habituated to the test environment for 30 min. Mechanical nociception was assessed using the up-down method with von Frey filaments³³. Mechanical sensitivity was evaluated using calibrated von Frey filaments (0.02–2.0 g). The first stimulus was always a 0.4-g filament. When a paw withdrawal reflex of the paw was elicited, the next lower-rated filament was applied, and when there was no response, the next higher-rated filament was used. After the first change in the response direction, four additional measurements were carried out, and the 50% withdrawal threshold was calculated using the up-down method³³.

Electrical stimulation-induced paw withdrawal test

The electrical stimulation-induced paw withdrawal test was performed as previously described²². Briefly, electrodes (3 mm in diameter) were attached to the left plantar and dorsal surfaces of the hind paws of each mouse. Transcutaneous nerve stimuli using each of three sine wave currents (5, 250, and 2000 Hz) were applied for 3 s through the electrodes. The current intensity increased gradually, and the minimum current intensity of the paw withdrawal response was defined as the paw withdrawal threshold. Transcutaneous nerve stimuli using each sine wave currents were applied to the paw at 5-min intervals.

Immunohistochemistry

Immunohistochemistry was performed as previously described³⁴. Briefly, mice were deeply anesthetized using sodium pentobarbital and then intracardially perfused with phosphate-buffered saline (PBS) followed by 4% paraformaldehyde in 0.1 M phosphate buffer (pH 7.4). The lumbar spinal cord was dissected, fixed in 4%

paraformaldehyde overnight, and cryoprotected in 30% sucrose overnight. Spinal cord sections (40 μm thick) were prepared using a sliding microtome. The free-floating spinal cord was blocked with PBS containing 10% normal goat serum and 0.2% Triton X-100 and then incubated with primary antibodies overnight. The primary antibodies included rabbit anti-c-Fos (1:1000, Cell Signaling Technology, Danvers, MA, USA #2250), and guinea pig anti-protein kinase C γ (PKC γ , 1:250, Frontier Institute, Hokkaido, Japan, #AB2571826). The immune complexes were visualized using Alexa 546-labeled anti-rabbit IgG (1:1000, ThermoFisher Scientific, Waltham, MA, USA #A11035), and Alexa 488-labeled anti-guinea pig IgG (1:800, Jackson ImmunoResearch Laboratories, West Grove, PA, USA, #706-545-148) secondary antibodies. Digital images were captured using a Nikon A1 laser-scanning confocal microscope equipped with an argon HeNe1 laser and appropriate filter (Nikon Corporation, Tokyo, Japan). Sections of the spinal cord were concurrently immunostained, and images were captured under the same conditions. c-Fos-positive cells were counted using the NIH ImageJ software. Background intensity (arbitrary units) was measured in the white matter area of the spinal cord. A cell was counted as positive cells if its intensity level was at least twice that of the background intensity level and if a single cell body was clearly defined. c-Fos immunoreactivity was quantified in 4–5 sections from each mouse ($n = 3$ mice). The numbers of positive cells from each mouse were expressed as the mean \pm S.E.M of the number in the indicated area (laminae I, II, and III–V) of the half spinal dorsal horn image.

Quantitative real-time PCR

Total RNAs were extracted from mouse tissues using TRIzol reagent (ThermoFisher Scientific), and the first-strand cDNA was synthesized from 0.8 μg of total RNA by using a ReverTra Ace (Toyobo, Osaka, Japan). First-strand cDNA was amplified in a GoTaq qPCR master mix (Promega, Madison, WI, USA) with specific primers, and the amplified products were detected with a QuantStudio 1 real-time PCR system (Applied Biosystem, Waltham, MA, USA). The sequences of primers were as follows: 5'-TTCCCGCCTCCAGATTCTTT-3' and 5'-CAAAGCAGGGTCAGGAGAGA-3' for TLR5; 5'-TCATTGCTCTCATGGGCGAGACTG-3' and 5'-TATGCC TATCTCGAGTGCTTGCCT-3' for TRPV1; 5'-AACTTGGCATTGTGGAAGG-3' and 5'-ACACATTGGGGG TAGGAACA-3' for glyceraldehyde-3-phosphate dehydrogenase (GAPDH)³⁵. The real-time PCR-amplifications were performed as follows: 1 cycle at 95 °C for 10 min followed by 40 cycles at 95 °C for 15 s and 60 °C for 1 min. The relative mRNA levels were calculated from the threshold cycle (Ct) values according to the $\Delta\Delta\text{Ct}$ method. The Ct values were normalized to those of GAPDH, as an internal control.

Statistical analysis

Statistical analyses were performed using Prism 8 (GraphPad Software Inc., La Jolla, CA, USA). Statistical analysis was performed using the unpaired Student's *t*-test (two-tailed) for comparisons between the two groups. Group means were compared using a one-way ANOVA with a post hoc Tukey's multiple comparison test and two-way repeated measures ANOVA with a post hoc Bonferroni test. Differences were considered statistically significant at $P < 0.05$. Data are expressed as the mean \pm S.E.M.

Data availability

The datasets generated in this study are available from the corresponding author on reasonable request.

Received: 4 July 2023; Accepted: 21 October 2023

Published online: 28 October 2023

References

- Bristow, J., Carey, W., Egging, D. & Schalkwijk, J. Tenascin-X, collagen, elastin, and the Ehlers–Danlos syndrome. *Am. J. Med. Genet. C Semin. Med. Genet.* **139C**, 24–30 (2005).
- Burch, G. H. *et al.* Tenascin-X deficiency is associated with Ehlers–Danlos syndrome. *Nat. Genet.* **17**, 104–108 (1997).
- Demirdas, S. *et al.* Recognizing the tenascin-X deficient type of Ehlers–Danlos syndrome: a cross-sectional study in 17 patients. *Clin. Genet.* **91**, 411–425 (2017).
- Schalkwijk, J. *et al.* A recessive form of the Ehlers–Danlos syndrome caused by tenascin-X deficiency. *N. Engl. J. Med.* **345**, 1167–1175 (2001).
- Voermans, N. C. *et al.* Neuromuscular involvement in various types of Ehlers–Danlos syndrome. *Ann. Neurol.* **65**, 687–697 (2009).
- Chopra, P. *et al.* Pain management in the Ehlers–Danlos syndromes. *Am. J. Med. Genet. C Semin. Med. Genet.* **175**, 212–219 (2017).
- Okuda-Ashitaka, E. & Matsumoto, K.-I. Tenascin-X as a causal gene for classical-like Ehlers–Danlos syndrome. *Front. Genet.* **14**, 1107787. <https://doi.org/10.3389/fgene.2023.1107787> (2023).
- Voermans, N. C., Knoop, H., Bleijenbergh, G. & van Engelen, B. G. Pain in Ehlers–Danlos syndrome is common, severe, and associated with functional impairment. *J. Pain Symptom Manage.* **40**, 370–378 (2010).
- Okuda-Ashitaka, E. *et al.* Mechanical allodynia in mice with tenascin-X deficiency associated with Ehlers–Danlos syndrome. *Sci. Rep.* **10**, 6569. <https://doi.org/10.1038/s41598-020-63499-2> (2020).
- Xu, Z. Z. *et al.* Inhibition of mechanical allodynia in neuropathic pain by TLR5-mediated A-fiber blockade. *Nat. Med.* **21**, 1326–1331 (2015).
- Binshtok, A. M., Bean, B. P. & Woolf, C. J. Inhibition of nociceptors by TRPV1-mediated entry of impermeant sodium channel blockers. *Nature* **449**, 607–610 (2007).
- Katims, J. J. Neuroselective current perception threshold quantitative sensory test. *Muscle Nerve* **20**, 1468–1469 (1997).
- Koga, K. *et al.* Selective activation of primary afferent fibers evaluated by sine-wave electrical stimulation. *Mol. Pain* **1**, 13. <https://doi.org/10.1186/1744-8069-1-13> (2005).
- Hunt, S. P., Pini, A. & Evan, G. Induction of c-fos-like protein in spinal cord neurons following sensory stimulation. *Nature* **328**, 632–634 (1987).
- Ji, R. R., Befort, K., Brenner, G. J. & Woolf, C. J. ERK MAP kinase activation in superficial spinal cord neurons induces prodynorphin and NK-1 upregulation and contributes to persistent inflammatory pain hypersensitivity. *J. Neurosci.* **22**, 478–485 (2002).
- Gao, Y. J. & Ji, R. R. c-Fos and pERK, which is a better marker for neuronal activation and central sensitization after noxious stimulation and tissue injury?. *Open Pain J.* **2**, 11–17 (2009).

17. Tashima, R. *et al.* Optogenetic activation of non-nociceptive A β Fibers induces neuropathic pain-like sensory and emotional behaviors after nerve injury in rats. *eNeuro* <https://doi.org/10.1523/ENEURO.0450-17.2018> (2018).
18. Neumann, S., Braz, J. M., Skinner, K., Llewellyn-Smith, I. J. & Basbaum, A. I. Innocuous, not noxious, input activates PKC γ interneurons of the spinal dorsal horn via myelinated afferent fibers. *J. Neurosci.* **28**, 7936–7944 (2008).
19. Tochitsky, I. *et al.* Inhibition of inflammatory pain and cough by a novel charged sodium channel blocker. *Br. J. Pharmacol.* **178**, 3905–3923 (2021).
20. Rosenbaum, T. & Simon, S. A. TRPV1 receptors and signal transduction. In *TRP Ion Channel Function in Sensory Transduction and Cellular Signaling Cascades Chapter 5* (eds Liedtke, W. B. & Heller, S.) (Taylor Francis, 2007).
21. Tominaga, M. The role of TRP channels in thermosensation. In *TRP Ion Channel Function in Sensory Transduction and Cellular Signaling Cascades Chapter 20* (eds Liedtke, W. B. & Heller, S.) (Taylor & Francis, 2007).
22. Fuseya, S. *et al.* Systemic QX-314 reduces bone cancer pain through selective inhibition of transient receptor potential vanilloid subfamily 1-expressing primary afferents in mice. *Anesthesiology* **12**, 204–218 (2016).
23. Zheng, X. Q., Wu, Y. H., Huang, J. F. & Wu, A. M. Neurophysiological mechanisms of cancer-induced bone pain. *J. Adv. Res.* **35**, 117–127 (2021).
24. van Dijk, F. S., Ghali, N., Demirdas, S. & Baker, D. TNXB-related classical-like Ehlers–Danlos syndrome. in *GeneReviews*[®] [Internet] (eds Adam, M. P. *et al.*). <https://www.ncbi.nlm.nih.gov/books/NBK584019/> (2022)
25. Voermans, N. C. *et al.* Mild muscular features in tenascin-X knockout mice, a model of Ehlers–Danlos syndrome. *Connect. Tissue Res.* **52**, 422–432 (2011).
26. Amir, R. & Devor, M. Functional cross-excitation between afferent A- and C-neurons in dorsal root ganglia. *Neuroscience* **95**, 189–195 (2000).
27. Attal, N. & Bouhassira, D. Mechanisms of pain in peripheral neuropathy. *Acta. Neurol. Scand. Suppl.* **173**, 12–24 (1999).
28. Brannagan, T. H. III. Peripheral neuropathy pain: mechanisms and treatment. *J. Clin. Neuromuscul. Dis.* **5**, 61–71 (2003).
29. Ueda, H. Peripheral mechanisms of neuropathic pain—Involvement of lysophosphatidic acid receptor-mediated demyelination. *Mol. Pain* **4**, 11. <https://doi.org/10.1186/1744-8069-4-11> (2008).
30. Caterina, M. J. *et al.* Impaired nociception and pain sensation in mice lacking the capsaicin receptor. *Science* **288**, 306–313 (2000).
31. Matsumoto, K. *et al.* Tumour invasion and metastasis are promoted in mice deficient in tenascin-X. *Genes Cells* **6**, 1101–1111 (2001).
32. Gregus, A. M., Levine, I. S., Eddinger, K. A., Yaksh, T. L. & Buczynski, M. W. Sex differences in neuroimmune and glial mechanisms of pain. *Pain* **162**, 2186–2200 (2021).
33. Chaplan, S. R., Bach, F. W., Pogrel, J. W., Chung, J. M. & Yaksh, T. L. Quantitative assessment of tactile allodynia in the rat paw. *J. Neurosci. Methods* **53**, 55–63 (1994).
34. Okuda-Ashitaka, E. *et al.* Nocistatin, a peptide that blocks nociceptin action in pain transmission. *Nature* **392**, 286–289 (1998).
35. Miyagi, M. *et al.* Macrophage-derived inflammatory cytokines regulate growth factors and pain-related molecules in mice with intervertebral disc injury. *J. Orthop. Res.* **36**, 2274–2279 (2018).

Acknowledgements

The authors thank Kiyoshi Matsumura, Yoshihiro Ohmiya, Taketo Omori, Hidetoshi Fujita, and Masato Nishiwaki for helpful discussion. This work was supported by a JSPS KAKENHI grant JP17K09045 and JP23H02804 and Osaka Institute of Technology Research Projects Grants to E O-A.

Author contributions

E.O.-A. supervised the study and participated in the design of experimental design and manuscript preparation. H.K. and E.O.-A. performed the behavioral analyses. H.K. and S.U. performed the electrical stimulation-induced paw withdrawal tests. H.K. performed the immunohistochemistry. H.K., K.E., and R.Y. performed quantitative real-time PCR. K.K., T.M. and S.I. contributed to the critical discussions and edited the manuscript. K.M. reviewed and edited the manuscript. All authors have read and approved the final manuscript.

Competing interests

The authors declare no competing interests.

Additional information

Correspondence and requests for materials should be addressed to E.O.-A.

Reprints and permissions information is available at www.nature.com/reprints.

Publisher's note Springer Nature remains neutral with regard to jurisdictional claims in published maps and institutional affiliations.



Open Access This article is licensed under a Creative Commons Attribution 4.0 International License, which permits use, sharing, adaptation, distribution and reproduction in any medium or format, as long as you give appropriate credit to the original author(s) and the source, provide a link to the Creative Commons licence, and indicate if changes were made. The images or other third party material in this article are included in the article's Creative Commons licence, unless indicated otherwise in a credit line to the material. If material is not included in the article's Creative Commons licence and your intended use is not permitted by statutory regulation or exceeds the permitted use, you will need to obtain permission directly from the copyright holder. To view a copy of this licence, visit <http://creativecommons.org/licenses/by/4.0/>.

© The Author(s) 2023